

1 **A comparison of measured HONO uptake and release with**  
2 **calculated source strengths in a heterogeneous forest**  
3 **environment**

4  
5 M. Sörgel<sup>1\*</sup>, I. Trebs<sup>2</sup>, D. Wu<sup>3</sup>, and A. Held<sup>1,4</sup>

6 1 University of Bayreuth, Atmospheric Chemistry, Bayreuth, Germany

7 2 Luxembourg Institute of Science and Technology, Environmental Research and Innovation  
8 (ERIN) Department, Belvaux, Luxembourg

9 3 Max Planck Institute for Chemistry, Biogeochemistry Department, Mainz, Germany

10 4 Bayreuth Center of Ecology and Environmental Research, Bayreuth, Germany

11 \* now at 3

12  
13  
14  
15  
16  
17  
18  
19  
20  
21  
22 Corresponding author:

23 Matthias Sörgel  
24 Biogeochemistry Department  
25 Max Planck Institute for Chemistry  
26 P.O. Box 3060, 55020 Mainz, Germany  
27 ++49-(0)6131-305-6401  
28 m.soergel@mpic.de  
29 <http://www.mpic.de/>

1 Abstract

2

3 Vertical mixing ratio profiles of nitrous acid (HONO) were measured in a clearing and on the  
4 forest floor in a rural forest environment. For the forest floor, HONO was found to be  
5 predominantly deposited, whereas net deposition was dominating in the clearing only during  
6 nighttime and net emissions were observed during daytime. For selected days, net fluxes of  
7 HONO were calculated from the measured profiles using the aerodynamic gradient method.  
8 The emission fluxes were in the range of 0.02 to 0.07 nmol m<sup>-2</sup> s<sup>-1</sup>, and, thus were in the lower  
9 range of previous observations. These fluxes were compared to the strengths of postulated  
10 HONO sources. Laboratory measurements of different soil samples from both sites revealed  
11 an upper limit for soil biogenic HONO emission fluxes of 0.025 nmol m<sup>-2</sup> s<sup>-1</sup>. HONO  
12 formation by light induced NO<sub>2</sub> conversion was calculated to be below 0.03 nmol m<sup>-2</sup> s<sup>-1</sup> for  
13 the investigated days, which is comparable to the potential soil fluxes. Due to light saturation  
14 at low irradiance, this reaction pathway was largely found to be independent of light intensity,  
15 i.e. it was only dependent on ambient NO<sub>2</sub>.

16 We used three different approaches based on measured leaf nitrate loadings for calculating  
17 HONO formation from HNO<sub>3</sub> photolysis. While the first two approaches based on empirical  
18 HONO formation rates yielded values in the same order of magnitude as the estimated fluxes,  
19 the third approach based on available kinetic data of the postulated pathway failed to produce  
20 noticeable amounts of HONO. Estimates based on reported cross sections of adsorbed HNO<sub>3</sub>  
21 indicate that the lifetime of adsorbed HNO<sub>3</sub> was only about 15 min, which would imply a  
22 substantial renoxification. Although the photolysis of HNO<sub>3</sub> was significantly enhanced at the  
23 surface, the subsequent light induced conversion of the photolysis product NO<sub>2</sub> did not  
24 produce considerable amounts of HONO. Consequently, this reaction might occur via an  
25 alternative mechanism.

26 By explicitly calculating the HONO formation based on available kinetic data and simple  
27 parameterizations we showed that a) for low NO<sub>x</sub> the light induced conversion of NO<sub>2</sub> on  
28 humic acids is light saturated already in the early morning, b) HONO formation from  
29 photolysis of adsorbed HNO<sub>3</sub> should proceed via an alternative mechanism and c) estimates  
30 of HONO emissions from soil are very sensitive to mass transfer and acidic soils do not  
31 necessarily favour HONO emissions.

32

# 1 Introduction

Gaseous nitrous acid (HONO) may contribute up to ~ 80% to the primary formation of hydroxyl radicals (OH), which play a key role in the degradation of most air pollutants (Kleffmann et al., 2005, Kleffmann 2007; Volkamer et al., 2010). The source of OH radicals is the photolysis of HONO (R1):



The back reaction R2 consumes OH and regenerates HONO. R3 is typically a minor loss term for HONO (e.g., Su et al., 2008; Sörgel et al., 2011a; Oswald et al., 2014) and OH due to the low concentrations of both reaction partners. Solely considering R1 to R3 HONO is an OH radical reservoir as discussed for urban plumes (Lee et al., 2013). If R1 to R3 are in equilibrium, a photo stationary state (PSS) is established (e.g. Cox, 1974; Kleffmann et al., 2005). In case an additional efficient HONO loss term exists (e.g. deposition) (Harrison et al., 1996; Wong et al., 2011; Vandenboer et al., 2013), HONO formation would be a sink for OH radicals. For instance it was shown that plants (Schimang et al., 2006) and soils (Donaldson et al., 2014) efficiently take up HONO. However, if additional sources of HONO exist that exceed the loss terms; HONO is a source for OH radicals.

A well-known source of HONO is the heterogeneous disproportionation of NO<sub>2</sub>, forming HONO and HNO<sub>3</sub>:



Although reaction R4 is well-known, its mechanism is still unclear. A potential mechanism involving the dimer of NO<sub>2</sub> was proposed by Finlayson-Pitts and co-workers (Finlayson-Pitts et al., 2003), and has been further analysed using theoretical approaches (Miller et al., 2009; De Jesus Medeiros and Pimentel, 2011). This reaction was found to be too slow to explain daytime HONO mixing ratios well above the PSS (e.g., Kleffmann et al., 2005; Sörgel et al., 2011a; Wong et al. 2013). However, it is linked to the nighttime accumulation of HONO, which triggers early morning photochemistry (Alicke et al., 2003). Other light-independent mechanisms for NO<sub>2</sub> conversion to HONO, such as the reduction by organics (Gutzwiller et al., 2002) and chemisorption on mineral surfaces (Gustafsson et al., 2008) were also

1 proposed. All these reactions have not yet been quantified under field conditions and concerns  
2 exist whether or not chemisorption would take place under environmental conditions  
3 (Finnlayson-Pitts, 2009). Furthermore, NO<sub>2</sub> reduction on soot was found to be quickly  
4 deactivated (Kleffmann et al., 1999; Arens et al., 2001; Aubin and Abbatt, 2007).

5 As the observed HONO mixing ratios almost always exceed those calculated from the PSS  
6 assumption (summarized by Kleffmann (2007) and Volkamer et al. (2010)), numerous  
7 attempts to identify HONO sources driven by light or by temperature that can overcome the  
8 loss by photolysis were made. Recently, it was found that the heterogeneous  
9 disproportionation (R4) can be catalysed by anions that are formed during photooxidation in  
10 the atmosphere (Yabushita et al., 2009; Colussi et al., 2013). Lightenhancement of R4 has  
11 also been attributed to HNO<sub>3</sub> photolysis (Ramazan et al., 2004), and photolysis of adsorbed  
12 HNO<sub>3</sub> on natural surfaces was proposed as an important HONO source in the atmosphere  
13 (Zhou et al., 2002; Zhou et al., 2003; Zhou et al., 2011).

14 In contrast to HONO formation observed on natural surfaces (Zhou et al., 2003, Zhou et al.,  
15 2011), HONO has not been detected as a primary reaction product of HNO<sub>3</sub> photolysis in  
16 laboratory studies up to now (Zhu et al., 2010, Schuttlefield et al., 2008, Rubasinghege and  
17 Grassian, 2009; Abida et al., 2012). Most studies (Zhu et al., 2010, Schuttlefield et al., 2008,  
18 Abida et al., 2012) report NO and NO<sub>2</sub> as the main products of this reaction (Rubasinghege  
19 and Grassian, 2009). The formation of NO<sub>2</sub> and NO<sub>2</sub>\* is also proposed for an alternative  
20 mechanism, which involves photolysis of complexes of either HNO<sub>3</sub> or NO<sub>3</sub><sup>-</sup> and NO<sub>2</sub> or  
21 N<sub>2</sub>O<sub>4</sub>, respectively (Kamboures et al., 2008). Recent studies applying a novel laser-based  
22 technique (Zhu et al., 2010, Abida et al., 2012) identified excited NO<sub>2</sub>\* as the main photolysis  
23 product of adsorbed HNO<sub>3</sub>, and, furthermore confirmed an enhanced absorption cross section  
24 of adsorbed HNO<sub>3</sub> compared to gas phase HNO<sub>3</sub>. Potentially, NO<sub>2</sub>\* reacting with water  
25 vapour can produce HONO, but this reaction does not result in significant amounts of HONO  
26 under atmospheric conditions (Crowley and Carl 1997; Sörgel et al., 2011a; Amedro et al.,  
27 2011). Hence, Zhou et al. (2011) suggested that NO<sub>2</sub> formed during HNO<sub>3</sub> photolysis further  
28 reacts via the mechanism proposed by Stemmler and co-workers (Stemmler et al., 2006;  
29 Stemmler et al., 2007), where solid organic material like humic acids (HA) acts as a  
30 photosensitizer and reduces NO<sub>2</sub> (George et al., 2005). Photosensitized reactions may be a  
31 promising pathway for explaining daytime HONO formation as hypothesized from  
32 correlations of the unknown HONO source with the photolysis frequency of NO<sub>2</sub>,  $j(\text{NO}_2)$ , or  
33 irradiance (e.g. Su et al., 2008; Sörgel et al., 2011a; Wong et al., 2012). The photolysis of o-

1 nitrophenols was also proposed as a HONO source (Bejan et al., 2006) that, however, has not  
2 yet been quantified in field measurements. As it depends on the amount of nitrophenols in air,  
3 this source is expected to be more important for polluted urban conditions (Bejan et al., 2006).  
4 A process directly driven by temperature could be the volatilization of HONO from soil nitrite  
5 (Kubota and Asami, 1985; Su et al. 2011). The temperature dependence of this process has  
6 been attributed to the temperature dependence of the Henry's law equilibrium between soil-  
7 solution and soil-air (Su et al., 2011). Additionally, it was suggested that HONO emissions  
8 are driven by ammonia oxidizing bacteria in soil, whose activity also depends on temperature  
9 (Oswald et al., 2013). Nitrogen availability for microorganisms was found as a limiting factor  
10 for HONO emissions from natural soils (Malianen et al., 2013). HONO deposition during  
11 night and reemission that is driven by acid displacement (VandenBoer et al. 2015) during  
12 daytime has been proposed to explain the missing daytime source (VandenBoer et al. 2013).  
13 The physicochemical interactions with soil particles have been analysed in more detail by  
14 Donaldson et al. (2014 a, b).

15 Regardless of the mechanism, the ground surface has been proposed as a major source of  
16 HONO (e.g. Febo et al., 1996; Stutz et al., 2002; Zhang et al., 2009; Sörgel et al., 2011b;  
17 Wong et al., 2012, Wong et al. 2013, VandenBoer et al., 2013), although there is a potential  
18 contribution from other heterogeneous sources within the boundary layer (Zhang et al., 2009;  
19 Wong et al., 2013). Flux measurements of HONO (Zhou et al., 2011; Ren et al., 2011)  
20 reported strong daytime upward fluxes, thus confirming a ground source. Contrarily, a recent  
21 study (Li et al., 2014) based on concentration measurements of HONO in the residual layer  
22 and the mixed layer proposed that an internal recycling mechanism (reaction between  $\text{NO}_x$   
23 and  $\text{HO}_x$ ) is mainly responsible for HONO formation.

24 In this study, we present vertical mixing ratio profiles of HONO measured close to the ground  
25 surface ( $< 2$  m) in a clearing and on the forest floor in a heterogeneous forest landscape in  
26 order to identify sources and sinks of HONO in natural environments. Under favourable  
27 conditions, our setup can be used to derive estimates of the surface fluxes of HONO by the  
28 aerodynamic gradient method. These fluxes are compared to best estimates of HONO source  
29 strengths of three proposed mechanisms derived from measured quantities: a) soil HONO  
30 emissions, b) photosensitized  $\text{NO}_2$  conversion, and c)  $\text{HNO}_3$  photolysis.

31

## 2 Experimental

Vertical mixing ratio profiles of HONO, nitrogen oxides ( $\text{NO}_x$ ), and ozone were measured in a clearing and on the forest floor at the Waldstein ecosystem research site in the Fichtelgebirge mountains, NE Bavaria (Germany) in 2011 and 2012 as part of the research project “Exchange processes in mountainous regions (EGER),” Foken et al. (2012). The profile measurements were made in June/July 2011 (intensive observation period IOP-3) in the clearing “Köhlerloh” (50°08'22.3" N, 11°52'01.5" E), and in August/September 2012 (IOP-4) on the forest floor about 290 m north of the clearing site close to the main tower (50°08'31.2" N, 11°52'00.8" E; 775 m a.s.l.) of the “Weidenbrunnen” site. Meteorological variables for the comparison of both campaigns were taken from the “Pflanzgarten” site, which is 280 m north-west of the main tower and 490 m north north-west of the clearing site. An aerial view of the different sites can be found in the Supplement (Fig. S1).

HONO was measured using a commercially available long path absorption photometer (LOPAP, QUMA, Wuppertal, Germany) with a time resolution of 3 minutes. A detailed description of the instrument is provided by Heland et al. (2001) and Kleffmann et al. (2002). The instrument was placed on a scaffold in a ventilated aluminium box as described by Sörgel et al. (2011b). The limit of detection ( $3\sigma$  of zero air noise) ranged from 1 to 7 ppt. NO and  $\text{NO}_2$  were measured by chemiluminescence (Model 42i-TL Thermo Scientific, Franklin, MA, USA) using a specific photolytic converter for  $\text{NO}_2$  (Droplet Measurement Technologies, Boulder, Co, USA). The limit of detection was 50 ppt for NO and about 140 ppt for  $\text{NO}_2$ . Trace gas profiles of HONO, NO, and  $\text{NO}_2$  were obtained by moving the external sampling unit of the LOPAP and an inlet line for  $\text{NO}_x$  to five (0.1 m, 0.2 m, 0.4 m, 0.8 m and 1.6 m) or three (0.1 m, 0.4 m and 1.6 m) different heights using an automated lift system (Fig. S2). The dwell time at each height was 6 and 7 min in IOP-3 and 9 min (IOP-4), which allowed sufficient sampling periods with respect to the time resolution of the LOPAP (1-2 data points). All data of the lift system ( $\text{NO}_x$ , HONO, temperature and lift position) were recorded every 20 sec. Additionally, eddy covariance measurements were made during IOP-3 with a CSAT3 sonic anemometer (Campbell Scientific, Logan, UT, USA) located at a height of 2.25 m on a mast about 20 m north-west of the profile measurements. During IOP-4, a Young sonic anemometer (Model 81000, R.M. Young, Traverse City, MI, USA) was located about 2 m east of the profile measurements at a height of 2 m. The friction velocity ( $u^*$ ) was calculated with the TK3 software (Mauder and Foken, 2011). Air temperature was measured

1 by radiation shielded and ventilated Pt-100 sensors with a resolution of 0.1 K at 1.4 m (1.6 m  
2 in IOP-4) and 0.1 m above ground level. Soil temperature was monitored with a Pt-100 sensor  
3 at a depth of 2 cm.

4 At the “Pflanzgarten” site, air temperature and relative humidity (RH) were measured with  
5 HMP45 sensors (Vaisala, Helsinki, Finland) at a height of 2 m, precipitation was measured  
6 with an OMC-212 rain gauge (Observator instruments, Ridderkerk, The Netherlands), and  
7 solar global irradiance was measured on the roof of the measurement container with a CM5  
8 pyranometer (Kipp and Zonen, Delft, The Netherlands). The HONO photolysis frequency  
9  $j(\text{HONO})$ , was calculated from global radiation according to Trebs et al. (2009).

10 Spectral irradiance and photolysis frequencies were calculated using the Tropospheric  
11 Ultraviolet and Visible (TUV) radiation model (Madronich and Flocke, 1998) version 5.0.  
12 Additional information about methods and instruments can be found in the supplementary  
13 material.

14

## 15 **3 Results and discussion**

### 16 ***3.1 Meteorological conditions and comparison of sites***

17

18 As shown in Fig. 1, the range of air temperature at the “Pflanzgarten” site was comparable for  
19 both campaigns and ranged between about 5 °C and 27 °C. The maximum temperatures were  
20 27.3 °C for IOP-3 and 25.8 °C for IOP-4, respectively. The minimum temperature of the  
21 June/July period (IOP-3) was lower (5.5 °C) than during IOP-4 in September (6.0 °C). Mean  
22 values (and standard deviations) were  $14.7 \pm 5.1$  °C for IOP-3 and  $14.2 \pm 4.4$  °C for IOP-4.  
23 Accordingly, RH values cover similar ranges from about 30 % to 100 % with somewhat  
24 higher values in the summer campaign due to frequent rain events (i.e. an average  
25 precipitation of  $1.8 \text{ mm d}^{-1}$  in IOP-3 and  $0.3 \text{ mm d}^{-1}$  in IOP-4). The long-term monthly means  
26 (1971-2000) at this site are  $3.6 \text{ mm d}^{-1}$  for June,  $4.1 \text{ mm d}^{-1}$  in July and  $2.8 \text{ mm d}^{-1}$  in  
27 September (Foken, 2003). Consequently, both periods exhibited less precipitation than the  
28 long term average, although frequent but light rain events occurred during IOP-3, whereas in  
29 September (IOP-4) precipitation events were rare. Maximal RH values are slightly different  
30 for the two IOPs and range from 95 % to ~ 100 %. The values greater than 100 % have to be  
31 viewed with caution as the sensor accuracy in the range from 90 % RH to 100 % RH is  $\pm 3$  %  
32 and the sensor is not able to measure accurately if water is condensing at high humidity.

1 Global radiation, and thus  $j(\text{HONO})$ , were higher in June/July 2011 than in September 2012.  
2 Correspondingly, the calculated  $j(\text{HONO})$  values show a maximum of  $2 \times 10^{-3} \text{ s}^{-1}$  in 2011 and  
3  $1.8 \times 10^{-3} \text{ s}^{-1}$  in 2012. The radiation and photolysis frequencies at the forest floor are a factor  
4 of 10 to 40 lower than above the canopy depending on the time of day and canopy structure  
5 (Sörgel et al., 2011b).  $J(\text{HONO})$  values calculated by applying a factor of 10 are shown in  
6 Fig. 1d. Since weather conditions were comparable, major differences between the two  
7 campaigns are expected to be due to a) availability of radiation, b) turbulent exchange and c)  
8 groundcover. Radiation and turbulent exchange are reduced at the forest site below the  
9 canopy compared to the open clearing. The ground cover at the clearing was dominated by  
10 grass and blueberry, while the forest floor was mainly covered by moss.

11

### 12 **3.2 HONO mixing ratio differences and estimated net fluxes**

13

14 NO mixing ratios at the 1.6 m level were generally low, especially during nighttime. Average  
15 mixing ratios were 0.2 ppb during the first period in 2011 (Fig. 2a), 0.1 ppb during the second  
16 period in 2011 (Fig. 2b), and 0.05 ppb in 2012 (Fig. 3a). Due to the well-known soil NO  
17 emissions (e.g., Ludwig et al., 2001; Bargsten et al., 2010) caused by microbiological activity,  
18 NO mixing ratios were higher at 0.1 m. The average mixing ratios close to the ground (Figs.  
19 S3 to S5) at 0.1 m were 0.75 ppb during the first period, 0.5 ppb during the second period in  
20 2011, and 0.1 ppb in 2012. Average NO<sub>2</sub> mixing ratios at the upper level were 1.7 ppb (min.  
21 0.3 ppb and max. 3 ppb) during the first period, 1.1 ppb (min. 0.2 ppb and max. 2.4 ppb)  
22 during the second period in 2011, and 1.6 ppb (min. 0.2 ppb and max. 4.8 ppb) in 2012.  
23 Average HONO mixing ratios at the 1.6 m level were 94 ppt (min. 12 ppt and max. 308 ppt)  
24 during the first period, 80 ppt (min. 30 ppt and max. 316 ppt) during the second period in  
25 2011, and 90 ppt (min. 26 ppt and max. 257 ppt) in 2012.

26 Since vertical mixing ratio differences are the result of the competition between sources and  
27 sinks as well as of transport dynamics, Fig. 2 and Fig. 3 additionally show vertical  
28 temperature differences and the friction velocity  $u^*$ . Temperature differences reflect  
29 atmospheric stability and  $u^*$  is a measure of the intensity of turbulent exchange. A typical  
30 diurnal cycle caused by radiative heating and cooling of the surface was observed at the  
31 clearing, with stable conditions (positive temperature differences) during the night and  
32 unstable conditions during the day. The temperature differences between 0.1 m and 1.4 m



1 above the ground were up to 6 K during the night and up to -4 K during the day. During stable  
2 conditions,  $u^*$  dropped and mixing ratio differences increased due to suppressed transport. In  
3 the clearing, very stable and calm conditions caused large HONO and NO (not shown) mixing  
4 ratio differences during sunset. Below the canopy at the forest site, diurnal cycles of stability  
5 are typically opposite to those observed at the clearing (Foken, 2008). However, the observed  
6 temperature differences do not feature a clear diurnal pattern and differences are generally an  
7 order of magnitude lower than at the clearing. This can be explained by the reduced heating of  
8 the forest floor and the reduced radiative cooling due to the shading of the canopy. As  
9 windspeed is reduced by the canopy as well, the friction velocity is on average a factor of  
10 three to four lower. Maximal values of  $u^*$  were  $0.46 \text{ m s}^{-1}$  in the clearing and  $0.16 \text{ m s}^{-1}$  on the  
11 forest floor, respectively. HONO differences in the clearing (1.6 m to 0.1m) shown in Figs.  
12 2c,d feature distinct diurnal cycles with positive gradients at night indicating net deposition  
13 and negative gradients during day indicating net emission. On the forest floor, HONO  
14 differences were either positive or close to zero, i.e. net emission was not observed (Fig. 3b).

15

16 We calculated net HONO fluxes from selected profiles using the aerodynamic gradient  
17 technique (cf. Wolff et al., 2010). Despite the fact that  $u^*$  was measured at 2.25 m on a  
18 separate tower about 20 m from the profile measurements at the clearing, the measurements  
19 were influenced by the same ground cover (dimensions of clearing  $\sim 300 \times 400 \text{ m}$ ). At the  
20 forest floor both measurements were collocated ( $\sim 2 \text{ m}$  distance and  $u^*$  measured in 2 m  
21 height). Mixing ratio differences were considered to be representative for the air layer  
22 between 1.6 m and 0.1 m at the forest floor, but at the clearing differences between 1.6 m and  
23 0.4 were taken as 0.1 m was below the zero plane displacement height (d).

24 The calculated daytime net emission fluxes of HONO at the clearing were in the range of 0.01  
25 to  $0.07 \text{ nmol m}^{-2} \text{ s}^{-1}$  (mean  $0.04 \pm 0.02 \text{ nmol m}^{-2} \text{ s}^{-1}$ ;  $N=17$ ). This is about a factor of three  
26 lower than fluxes reported for another rural forested site (Zhou et al., 2011; Zhang et al.,  
27 2012) and about an order of magnitude lower than for semi-rural and urban sites (Harrison  
28 and Kitto 1994; Harrison et al. 1996; Ren et al., 2011). However, these fluxes are higher than  
29 the values observed at Blodgett Forest (Ren et al., 2011). The mean HONO net emission flux  
30 estimate of  $0.04 \text{ nmol m}^{-2} \text{ s}^{-1}$  with a corresponding mixing ratio of 65 ppt at 1.6 m at the  
31 clearing compares reasonably well with the somewhat lower fluxes at Blodgett Forest (flux  $<$   
32  $0.01 \text{ nmol m}^{-2} \text{ s}^{-1}$ ; 20-30 ppt) and with the somewhat higher fluxes at the PROPHET site  
33 (mean flux  $0.19 \text{ nmol m}^{-2} \text{ s}^{-1}$ ; 70 ppt). The low fluxes at Blodgett Forest have been attributed

1 to the alkalinity of the soil, which, according to acid- base and Henry's Law equilibrium (Su et  
2 al., 2011), should enhance HONO uptake or hinder the release. The calculated fluxes indicate  
3 the existence of a daytime ground source, whose strength is comparable in order of magnitude  
4 to that found in other studies in rural forested areas. Nighttime net deposition fluxes ( $0.006 \pm$   
5  $0.003 \text{ nmol m}^{-2} \text{ s}^{-1}$ ; N = 12) were about a factor of seven lower than daytime net emission  
6 fluxes at the clearing (see Sect. 3.3.1).

7 At the forest floor, only net deposition was observed with fluxes varying between zero and  
8 about  $0.012 \text{ nmol m}^{-2} \text{ s}^{-1}$  (mean:  $0.004 \pm 0.003$ ; N = 52) for the selected days (4 -7 Sep 2012).  
9 Hence, net deposition fluxes at the forest floor were comparable to nighttime net deposition at  
10 the clearing. Assuming that daytime deposition fluxes at the clearing are within the same  
11 range, emission fluxes at the clearing are at least about 15 % higher than the net fluxes. If  
12 considerable stomatal uptake of HONO, as proposed by Schimang et al. (2006), occurs, the  
13 daytime deposition would be much higher than during nighttime due to stomatal aperture.  
14 Hence, to sustain the observed net emission fluxes, the HONO emission from the ground  
15 would be even higher.

16 It should be noted that the derived fluxes should be considered as rough estimates for several  
17 reasons. The profiles were measured sequentially and not simultaneously at the different  
18 heights. Hence, only profiles under stationary conditions were evaluated, i.e. when mixing  
19 ratio changes between two profile cycles were small at each measurement height. This was  
20 mainly the case from 22:00 to 4:00 during night and from 11:00 to 15:00 during day.  
21 Furthermore, the mixing ratio differences during daytime were rather small (5 to 26 ppt; mean  
22 14 ppt). The differences were 1.3 to 8.5 times the standard deviation of the mean values at one  
23 height and larger than the combined errors (sum of standard deviations of both heights).  
24 Differences that were smaller than the combined standard deviation were omitted for the flux  
25 calculations. Besides the uncertainty in the mixing ratio differences, the estimate of the zero-  
26 plane displacement height  $d$  has considerable influence on the fluxes. We used  $d = 0.7$  times  
27 the canopy height (Foken, 2008) with a canopy height of 0.25 m of the surrounding blueberry  
28 canopy (Falge, 2014 personal communication) at the clearing. As roughness elements (like  
29 dead wood, blueberry, small spruce and grass) were distributed very inhomogeneously, it is  
30 unclear if the applied displacement height is appropriate and would hold for all wind  
31 directions. If the canopy height would have been chosen as 0.4 m instead, the fluxes would  
32 decrease by about 20 %. Compared to the error of the mixing ratio differences and of the  
33 displacement height, the error in  $u^*$  is expected to be negligible. At the forest floor we

1 measured at a flat surface covered with moss that has a comparably low roughness ( $d = 0.007$   
2 m), thus the fluxes are less sensitive to small differences in  $d$ .

### 4 **3.3 HONO sinks**

#### 5 **3.3.1 Deposition**

6  
7 Except for the uptake of HONO by aerosol surfaces, no considerable gas phase HONO sinks  
8 exist in the absence of light. This implies that dry and wet deposition are the most important  
9 loss pathways in the dark.

10 Net deposition means that although HONO formation by either heterogeneous  
11 disproportionation of  $\text{NO}_2$  or direct soil emission may take place, net deposition is observed  
12 because the production of HONO is smaller than the loss by deposition. For our study, soil  
13 emissions can be neglected (see 3.4.1). Calculated nighttime deposition velocities of 0.08 to  
14  $0.5 \text{ cm s}^{-1}$  (mean  $0.24 \pm 0.13$ ) at the clearing were in the lower range of reported values at  
15  $0.08$  to  $6 \text{ cm s}^{-1}$  (Harrison and Kitto 1994; Harrison et al., 1996; Stutz et al., 2002).

16 At the forest floor, deposition was the dominating process during day and night. The vertical  
17 profiles (Fig. 3b) do not provide evidence that HONO emission from the ground surface takes  
18 place because the differences are either positive or ambiguous within the uncertainty range.  
19 The HONO deposition velocities ranged from 0.03 to 0.4 (mean  $0.16 \pm 0.08 \text{ cm s}^{-1}$ ), which is  
20 in the lower range of previously reported values (e.g., Harrison et al., 1996, Stutz et al., 2002)  
21 and a factor of 1.5 lower than at the clearing. To our knowledge, measured HONO fluxes at  
22 forest floors have not been reported up to now.

23 In a modelling study, Wong et al. (2011) pointed out that nighttime deposition is an important  
24 part of HONO cycling, which was recently confirmed by vertical profile measurements  
25 (VandenBoer et al., 2013). VandenBoer et al. (2013) proposed that the deposited HONO  
26 might form a reservoir that is re-emitted during the day, and, can thus explain a significant  
27 fraction of the missing daytime source. For the forest floor, we can exclude this pathway as a  
28 general source of HONO because no emissions were observed. This is in line with laboratory  
29 studies, which showed that HONO can be taken up by plants (Schimang et al., 2006) and soil  
30 (Donaldson et al., 2014). Due to the limited available data we cannot exclude that re-emission  
31 may occasionally take place. However, we showed that net deposition (even if it is small)  
32 persists during the day at the forest floor during our measurement period. Thus, sources and

1 sinks coexist over small spatial scales, which has to be taken into account for measurements at  
2 elevated levels that integrate over larger areas (horizontal heterogeneity), as well as for  
3 measurements above the canopy (vertical heterogeneity).  
4

### 5 **3.3.2 Photolysis**

6  
7 Photolysis has been identified as the dominating HONO loss process during the day (e.g.,  
8 Kleffmann, 2007; Su et al., 2008; Sörgel et al., 2011a; Wong et al., 2013; VandenBoer et al.,  
9 2013; Oswald et al., 2014). We calculated the HONO loss rates from photolysis frequencies  
10 and HONO mixing ratios within a boundary layer height of 1000 m in two different ways: (a)  
11 the measured HONO mixing ratio at 1.6 m was used for the entire volume or, (b) assuming a  
12 linear HONO profile throughout the boundary layer to account for elevated HONO levels  
13 close to the ground as observed by Zhang et al. (2009) and VandenBoer et al. (2013). The  
14 artificial linear HONO profile was created using the measurements at 1.6 m and a background  
15 level (free troposphere) of 10 ppt (Zhang et al., 2009). The geometric mean of these values  
16 was used to calculate the HONO loss within the boundary layer volume. Using these two  
17 simplified approaches yields loss rates of (a) 0.2-1 ppb h<sup>-1</sup> and (b) 0.08-0.5 ppb h<sup>-1</sup>. These  
18 values are within the range of values reported for the unknown HONO source (e.g. Kleffmann  
19 2007). This is not surprising because the photolytic loss and the unknown source were found  
20 to be the dominant terms of the HONO budget for low NO<sub>x</sub> levels (e.g., Sörgel et al., 2011a;  
21 Oswald et al., 2014), i.e. in the absence of other sources and sinks the photolytic loss equals  
22 the unknown source. Integrating the photolytic loss term over a boundary layer height of 1000  
23 m and converting it into a surface flux yields mean fluxes of (a) 4.6 nmol m<sup>-2</sup> s<sup>-1</sup> and (b)  
24 2 nmol m<sup>-2</sup> s<sup>-1</sup> respectively, which is a factor 100 and 40 higher than the mean emission flux  
25 derived from the measurements at the clearing (see Sect. 3.2). Consequently, the contribution  
26 of the surface emissions to the HONO source would be in the order of a few percent. This is  
27 in agreement with a proposed internal volume source (Li et al., 2014) and estimates of ground  
28 source contributions of about 20 % derived from measured boundary layer profiles (Zhang et  
29 al., 2009; Li et al., 2014). Close to the ground (lowest 35 m) a contribution of more than 60 %  
30 was found in modelling studies (Czader et al., 2012; Wong et al. 2013). As these studies were  
31 conducted in the urban area of Houston (Texas, USA), which is characterized by higher direct  
32 HONO emissions and higher levels of NO<sub>x</sub> compared to our site, the relative contribution of  
33 the ground source in the lowest 35 m might be higher for our site. Nevertheless, the  
12

1 contribution was reduced to about 50 % by integrating the lowermost 300 m (Wong et al.,  
2 2013), and, therefore integrating over a boundary layer height of 1000 m will further reduce  
3 this contribution. As none of the other boundary layer profile measurements have been  
4 analysed with a chemistry-transport model up to now, it remains unclear if the differences in  
5 HONO budgets (ground versus gas phase) are real or are caused by the different assumptions  
6 and simplifications in the different approaches.

### 8 **3.4 HONO ground sources**

9  
10 The existence of a HONO ground source was confirmed by profile (e.g., Zhang et al., 2009;  
11 VandenBoer et al., 2013) and flux measurements (Zhou et al., 2011; Ren et al., 2011). In the  
12 following we compare the measured ground source to estimates for three different proposed  
13 formation mechanisms based on measured quantities.

#### 14 **3.4.1 Soil emissions**

15  
16 For both the forest and the clearing site, a set of soil samples was collected from two different  
17 ground cover types and potential HONO emission fluxes were measured using a dynamic  
18 chamber in the laboratory (for details see Appendix). HONO fluxes were mostly within the  
19 calculated uncertainty range (Fig. S6). The sample taken directly below the lift system at the  
20 clearing (sample 4, Fig.S6) was the only sample for which potential emissions were observed.  
21 From those measurements we derive an upper limit for the HONO soil emission flux of  $0.025$   
22  $\pm 0.015$   $\text{nmol m}^{-2} \text{s}^{-1}$ . This flux also represents an upper limit with regard to the experimental  
23 conditions as the chamber was flushed with zero air and the samples were measured at 25 °C.  
24 During the field measurements, the soil temperature at 2 cm depth did not exceed 20 °C at the  
25 clearing. Comparison of the maximal fluxes measured in the laboratory ( $0.025$   $\text{nmol m}^{-2} \text{s}^{-1}$ )  
26 with maximal fluxes calculated from soil nitrite ( $0.35 - 0.99$   $\text{mg kg}^{-1}$  in terms of N) and pH  
27 ( $3.0 - 3.4$ ) values ( $F(\text{HONO}_{\text{max}}) = 1810$   $\text{nmol m}^{-2} \text{s}^{-1}$ ) according to Su et al. (2011) reveals that  
28 the measured fluxes are at least four orders of magnitude lower. For the calculations we used  
29 a gravimetric soil water content of  $\vartheta_{\text{soil}} = 0.2$   $\text{kg kg}^{-1}$ , a transfer velocity ( $v_{\text{tr}}$ ) of  $1$   $\text{cm s}^{-1}$  (Su et  
30 al., 2011) and measured pH and nitrite values (see Table S1). The discrepancy between our  
31 measurements and the calculations according to Su et al. (2011) reduces to about a factor of  
32 50 when  $v_{\text{tr}}$  is determined for our measurement setup instead of using a fixed value of  $1$   $\text{cm s}^{-1}$

1 <sup>1</sup>. The transfer velocity  $v_{tr}$  was determined by calculating the soil resistance according to  
2 Moldrup et al. (2000) from measured soil properties for the Waldstein site (Bargsten et al.,  
3 2010) and using the aerodynamic resistance ( $R_{aero} = 90 \text{ s m}^{-1}$ ) from a chamber system of  
4 similar design and dimensions (Pape et al., 2009). This comparison emphasizes the  
5 importance of explicitly considering mass transfer between the soil and atmosphere.  
6 Additionally, based on soil nitrite ( $\sim 1 \mu\text{g g}^{-1} \text{N}$ ) and pH ( $\sim 3$ ) values at our site, one would  
7 expect rather high HONO emissions according to the acid base and Henry's law equilibrium.  
8 Hence, it seems more likely that microbes are directly involved in the HONO formation as  
9 proposed by Oswald et al. (2013), but microbial activity in our samples was low due to the  
10 low pH ( $\sim 3$ ) of the organic soil (e.g., Matthies et al., 1997; de Boer and Kowalchuk, 2001  
11 and Rousk et al., 2010). Maljanen et al. (2013) found that some acidic forest soils emit  
12 measurable amounts of HONO and, thus, proposed nitrogen availability for the microbes as  
13 an important factor controlling HONO emissions. The mechanisms controlling HONO  
14 emissions from soils (microbial production versus physicochemical release) are still under  
15 debate. Maximum emissions for neutral to alkaline soils were attributed to the activity of  
16 ammonium oxidizing bacteria (Oswald et al. 2013). Donaldson et al. (2014b) studied the effect  
17 of surface acidity of soil particles (in contrast to the bulk soil pH) on HONO uptake. Their  
18 study confirmed that rather the acidity of the particles than the bulk pH determined the  
19 HONO exchange, which could explain HONO emissions at high (bulk) pH. Nevertheless, this  
20 mechanism is applicable to mineral soils only. Another possible effect would be HONO loss  
21 in the soil by chemodenitrification as proposed by Clark (1962). During chemodenitrification  
22 in the soil, HONO is converted to NO and N<sub>2</sub>O depending on pH and organic content with the  
23 highest conversion rates at low pH and high organic content (e.g. Allison 1963, van Cleemput  
24 and Baert 1984; Ventera et al., 2005). A recent flow tube study (Donaldson et al., 2014a)  
25 reports 16 % NO and 13 % N<sub>2</sub>O yield from HONO adsorbing to a mineral soil (less than 3 %  
26 organic and pH of 6.5). Thus, based on the prior semi quantitative studies high loss rates  
27 could be expected for the organic soil at our site. Therefore, the acidic conditions of the  
28 organic soil at the Waldstein site may lead to additional HONO loss by chemodenitrification  
29 and, thus, low soil HONO emissions.

30  
31

### 3.4.2 Light-induced NO<sub>2</sub> conversion

HONO fluxes from light-induced NO<sub>2</sub> conversion were calculated by assuming that the flux from the surface equals the chemical formation at the surface. HONO is formed by reactive collisions of NO<sub>2</sub> with the humic acid surface, and Stemmler et al. (2007) defined their uptake coefficient ( $\gamma_{rxn}$ ) as the ratio of these reactive collisions to the number of gas-kinetic collisions of NO<sub>2</sub> molecules with the surface. Hence, we calculated the HONO flux by multiplying the number of gas kinetic collisions given by Eq. (1) with the reactive uptake coefficient given by Eq. (2) (Stemmler et al., 2007):

$$Z_w = \frac{n \times \omega}{4} \quad (1)$$

$$\gamma_{rxn} = \frac{4}{\omega} \times \frac{1}{9.3 \times 10^{22} \times [NO_2] \times [F]^{-1} + 2330} \quad (2)$$

where  $Z_w$  is the number of collisions per time (s) and area (m<sup>2</sup>),  $n$  is the volume number density per m<sup>3</sup>,  $\omega$  is the mean thermal velocity of NO<sub>2</sub> in m s<sup>-1</sup>, [NO<sub>2</sub>] is the NO<sub>2</sub> mixing ratio in ppb measured at 10 cm above the surface, and  $F$  is the actinic flux in the 400-750 nm range in photons per m<sup>3</sup> and s<sup>-1</sup>. For simplicity, we used the irradiance in the 400-700 nm range (equivalent to the photosynthetic active radiation (PAR)) instead of the actinic flux from 400-750 nm for  $F$  because this value can be directly compared to measurements and to the model output of the TUV. Furthermore, in the study of Stemmler et al. (2007) the actinic flux of the lamps and absorption of the humic acid was low in the 700-750 nm wavelength range, thus having a small influence on the reactive uptake. Since our simple model assumes a flat surface of 1 m<sup>2</sup> completely covered with humic acid, it is well justified to use the irradiance instead of the actinic flux.

Calculation of the HONO flux using equations 1 and 2 with NO<sub>2</sub> mixing ratios measured 10 cm above the surface and modelled irradiance resulted in light-saturation of HONO formation in the early morning at about 7:00 CET and it remains independent of light intensity for most of the day (see Fig. 4). In addition, the saturation itself is dependent on NO<sub>2</sub> with the fastest saturation observed for low NO<sub>2</sub> mixing ratios. Stemmler et al. (2006) explain this behaviour by two competing processes: a) the light driven formation of the “reductive centres” that react with NO<sub>2</sub> and b) the competing light driven formation of oxidants that deactivate these reductive centres. If more NO<sub>2</sub> is available at the surface the reaction rate increases and the deactivation rate decreases. A saturation of the surface with respect to NO<sub>2</sub> is observed for

1 mixing ratios > 50 ppb (Stemmler et al., 2006; Stemmler et al., 2007). If this saturation  
2 behaviour (with respect to light intensities) also prevails on natural surfaces, at mixing ratios  
3 below 1 ppb the unknown HONO source should be solely correlated with NO<sub>2</sub> independent  
4 from radiation, which to our knowledge has not been reported up to now. Previous studies  
5 found that the unknown HONO source correlated with  $j(\text{NO}_2)$  or irradiance with only a minor  
6 dependence on NO<sub>2</sub> (e.g., Su et al., 2008; Sörgel et al., 2011a; Wong et al., 2012). However,  
7 the type and structure of photosensitizers on natural surfaces might differ substantially from a  
8 pure humic acid film and, thus, might not be saturated at high light intensities. For example  
9 for humic acid dissolved in ice, Bartels-Rausch et al. (2010) did not observe deactivation of  
10 the surface uptake. However, only actinic fluxes of up to about 100 W m<sup>-2</sup> (400-700 nm) were  
11 considered, compared to irradiance values of about 400 W m<sup>-2</sup> in the same wavelength range  
12 around noon in our study. Consequently, we consider the light saturation of NO<sub>2</sub> conversion  
13 on organic surfaces as a key issue for determining the role of this HONO formation pathway  
14 in the environment.

15

### 16 **3.4.3 Photolysis of adsorbed HNO<sub>3</sub>**

17

18 The photolysis of HNO<sub>3</sub> adsorbed to surfaces has also been suggested as a source of HONO  
19 (e.g., Zhou et al., 2002; Zhou et al., 2011). We measured the leaf nitrate loadings of young  
20 spruce trees (up to 1.6 m height) at the clearing close to the HONO measurement setup. A  
21 detailed description of the sampling and the calculations can be found in the supplementary  
22 material. Unfortunately, measurements of the nitrate loadings on the grass below the HONO  
23 inlets are not available, but we assume that they are comparable to the nitrate loadings of the  
24 trees. Nitrate loadings at the forest site were not measured, but the contribution of HNO<sub>3</sub>  
25 photolysis is expected to be much lower than at the clearing as the available radiation is  
26 attenuated by the canopy by a factor of about 10 – 25 (Sörgel et al., 2011b). Furthermore, we  
27 have found no evidence for a HONO source at the forest floor (cf. Sect. 3.2).

28 The nitrate loadings of the young spruce trees at the clearing are  $1.7 \pm 0.7 \times 10^{-5}$  mol m<sup>-2</sup>,  
29 which is in relatively good agreement with the value of  $0.8 \pm 0.3 \times 10^{-5}$  mol m<sup>-2</sup> reported by  
30 Zhou et al. (2011). Both research sites are located in rural forested areas, but considering the  
31 influence of different environmental variables, such as NO<sub>x</sub> mixing ratios, precipitation  
32 intensity and plant surfaces, all of which influence HNO<sub>3</sub> formation and deposition, a  
33 variation by a factor of two may be expected.



1 The potential HONO emission fluxes from the photolysis of adsorbed HNO<sub>3</sub> were calculated  
2 using three different approaches:

- 3 i) All measured nitrate represents adsorbed HNO<sub>3</sub> at the top surface of the needles, and  
4 HONO formation from photolysis of adsorbed HNO<sub>3</sub> proceeds with an empirical  
5 enhancement factor of 43 of  $j(\text{HNO}_3)$  (Zhou et al., 2011).
- 6 ii) Similar to i) but the nitrate loading is distributed over the whole geometric surface of  
7 the needles (Oren et al., 1986), thus, a factor of 2.65 less HNO<sub>3</sub> is exposed to  
8 radiation.
- 9 iii) The photolysis frequency of adsorbed HNO<sub>3</sub> is calculated directly from the absorption  
10 cross section of adsorbed HNO<sub>3</sub> on fused silica reported by Zhu et al. (2008) and the  
11 corresponding irradiance calculated by the TUV model. This photolysis frequency  
12 multiplied with the nitrate loading according to ii) yields the NO<sub>2</sub> formed at the  
13 surface. Then, HONO formation is calculated as described in Sect. 3.4.2. To derive the  
14 reactive uptake coefficient according to Eq. (2) (Stemmler et al., 2007) we used the  
15 irradiance integrated over the 290-700 nm wavelength range and calculated the NO<sub>2</sub>  
16 concentration which is equivalent to the amount of NO<sub>2</sub> molecules formed at the  
17 surface by HNO<sub>3</sub> photolysis.

18  
19 A comparison of  $j(\text{NO}_2)$  values from the TUV model with those calculated from global  
20 radiation measurements by the approach of Trebs et al. (2009) showed a reasonable  
21 agreement. The values agree within 8 % around noon.

22 Figure 5 summarizes the results of the different approaches. Based on empirical factors of  
23 light enhancement and HONO formation (Zhou et al., 2011) approaches i) and ii) yielded a  
24 light-dependent HONO source in the same order of magnitude as the estimated HONO fluxes  
25 ( $0.04 \pm 0.02 \text{ nmol m}^{-2} \text{ s}^{-1}$ ; see Sect. 3). The calculated potential HONO fluxes according to  
26 approach i) are a factor of two higher (about  $0.46 \text{ nmol m}^{-2} \text{ s}^{-1}$ ) than those of Zhou et al.  
27 (2011) ( $0.25 \text{ nmol m}^{-2} \text{ s}^{-1}$ ), which is consistent with the factor of two higher nitrate loading  
28 measured at our site. However, we consider approach ii) to be more realistic. The diurnal  
29 cycle of this source (Fig. 5) follows  $j(\text{HNO}_3)$  as the mean nitrate loading is used for the  
30 calculation. This seems to be valid as we found rather constant surface nitrate loadings during  
31 different times of the day (see Fig. S4).

1 Approach iii), a combination of photolysis of adsorbed HNO<sub>3</sub> and light-induced conversion of  
2 the photolysis product NO<sub>2</sub> (see also section 3.4.2) as proposed by Zhou et al. (2011), reveals  
3 several interesting findings:

- 4 • The calculated photolysis frequency of adsorbed HNO<sub>3</sub> is higher than in the gas phase  
5 by a factor of 2000.
- 6 • The lifetime of adsorbed HNO<sub>3</sub> with respect to photolysis is only about 15 min at  
7 noon.
- 8 • NO<sub>2</sub> formed at the surface by HNO<sub>3</sub> photolysis corresponds to a mixing ratio of NO<sub>2</sub>  
9 in the gas phase of only a few ppt.

10 If the strongly enhanced photolysis of adsorbed HNO<sub>3</sub> is valid for natural surfaces, this would  
11 have important implications for HNO<sub>3</sub> deposition. HNO<sub>3</sub> would most likely be an  
12 intermediate with a lifetime comparable to that of HONO (about 15 min at noon) than a final  
13 sink for NO<sub>x</sub>. However, even if photolysis of adsorbed HNO<sub>3</sub> is strongly enhanced, formation  
14 of HONO would be rather slow if the subsequent reaction of NO<sub>2</sub>\* (Abida et al., 2012) occurs  
15 via the light-induced NO<sub>2</sub> conversion (Stemmler et al., 2006) as proposed by Zhou et al.  
16 (2011). As shown in sect. 3.4.2 the light induced conversion is light saturated during most of  
17 the day especially for low NO<sub>2</sub> mixing ratios. If we compare the number NO<sub>2</sub> molecules  
18 formed at the surface through HNO<sub>3</sub> photolysis to the number of NO<sub>2</sub> molecules hitting the  
19 surface through gas kinetic collisions this would correspond to a mixing ratio of a few ppt  
20 only. Thus, this pathway would not compete with ambient NO<sub>2</sub> for the conditions in our  
21 study. Hence, a different NO<sub>2</sub>\* reaction mechanism to explain the proposed HONO formation  
22 from HNO<sub>3</sub> must exist. A potential pathway for NO<sub>2</sub>\* to form HONO would be the reaction  
23 with water (e.g., Crowley and Carl 1997; Amedro et al., 2011). Sörgel et al. (2011a)  
24 speculated that the reaction of NO<sub>2</sub>\* with water at the surface might be faster than the  
25 respective gas phase reaction, which is not of atmospheric importance (e.g., Crowley and Carl  
26 1997; Sörgel et al., 2011a; Amedro et al., 2011). The formation of NO<sub>2</sub>\* (either from HNO<sub>3</sub>  
27 photolysis or directly in the gas phase) is not the limiting step, as in the gas phase *j* values for  
28 excitation (NO<sub>2</sub> → NO<sub>2</sub>\*) are about a factor of five higher under typical tropospheric  
29 conditions (Crowley and Carl, 1997) than for photo dissociation of NO<sub>2</sub>. The limiting step is  
30 the small portion of reactive quenching of NO<sub>2</sub>\* by water vapour as the majority of excited  
31 NO<sub>2</sub> molecules gets deactivated by collision with N<sub>2</sub>, O<sub>2</sub> and water vapour. According to  
32 Abida et al. (2012), deactivation of NO<sub>2</sub>\* is much faster at the surface than in the gas phase,  
33 thus reducing the probability for reactive quenching with water and formation of HONO. For

1 a quantitative evaluation of this reaction pathway, knowledge of the ratio of deactivation to  
2 reactive quenching of surface adsorbed  $\text{NO}_2^*$  and  $\text{H}_2\text{O}$  is crucial. Another pathway might be  
3 the photolysis of nitrate in aqueous solution that has been reported to yield HONO and  $\text{NO}_2$   
4 (Scharko et al. 2014), whereby HONO formation was attributed to efficient hydrolysis of  $\text{NO}_2$   
5 that is formed in solution.

### 7 ***3.5 Comparison of calculated fluxes and source estimates***

8  
9 Transferring the HONO formation mechanisms proposed from laboratory measurements to  
10 field conditions involves uncertainties as discussed in detail in the previous sections.  
11 However, except for  $\text{HNO}_3$  photolysis (Zhou et al., 2011) these source mechanisms have not  
12 been quantified in field studies up to now. Furthermore, to our knowledge the various  
13 reactions have not been studied under natural conditions, except for a proof of principle with  
14 irradiated bare soil as a natural humic acid environment (Stemmler et al., 2006), and the  
15 empirically derived  $\text{HNO}_3$  conversion factors (Zhou et al., 2003). In Figure 6 all source  
16 estimates and the observed flux estimates from the field are summarized. The main findings  
17 are a) that all sources are within the same order of magnitude, and b) due to the large  
18 systematic uncertainties of the source estimates and the potentially large errors of the flux  
19 estimates, none of the sources can be favoured or excluded.

20 The soil flux was the only source to be measured directly, and these measurements were  
21 performed in the laboratory. The soil HONO flux would likely be lower in the field as the soil  
22 at the site was covered by vegetation which can take up HONO (Schimang et al., 2006) and  
23 because ambient HONO mixing ratios were above zero.  $\text{NO}_2$  mixing ratios dropped below  
24 500 ppt in the afternoon, leading to very low HONO fluxes from light-induced  $\text{NO}_2$   
25 conversion. Surprisingly, this photochemical source did not show a diurnal cycle but became  
26 light-saturated early in the morning and, thus, was solely dependent on  $\text{NO}_2$  mixing ratios. It  
27 remains an open question whether light saturation occurs also on natural surfaces. The  
28 photolysis of adsorbed  $\text{HNO}_3$  produced considerable HONO fluxes ((even for case ii), Sect.  
29 3.4.3) when using an empirically derived HONO conversion factor (Zhou et al., 2003; Zhou et  
30 al., 2011). In contrast, the proposed mechanism based on reaction kinetics ((case iii), Sect.  
31 3.4.3) failed to produce considerable amounts of HONO. Although some of the sources were  
32 unexpectedly small, the combination of all three sources yields much higher fluxes than  
33 measured in the field. This may be attributed to enhanced deposition of HONO during the day

1 due to stomata opening and take-up by plants (Schimang et al., 2006), which would reduce  
2 measured net emission fluxes. However, the contribution of daytime deposition has not been  
3 measured up to now.

## 4 **4 Conclusions**

5 Our results reveal that the forest floor was predominantly a net sink for HONO, and the  
6 clearing constitutes a net sink for HONO during nighttime and a net source during daytime.  
7 Hence, net sources and net sinks coexist in heterogeneous landscapes.

8 HONO emissions calculated for three proposed mechanisms agreed with the measured fluxes  
9 within one order of magnitude. On the one hand, this shows that the postulated sources are of  
10 the right order of magnitude, but on the other hand, even the presented comprehensive data  
11 set including vertical profiles is not sufficient to exclude or confirm one individual source.  
12 The detailed investigation of three potential HONO sources, i.e., soil emissions, NO<sub>2</sub>  
13 conversion with humic acids and photolysis of adsorbed HNO<sub>3</sub>, revealed important findings:

14

- 15 • Soil emissions were found to be several orders of magnitude lower than expected from  
16 the model of Su et al. (2011), and calculated fluxes are very sensitive to the  
17 parameterization of mass transfer from the soil to the atmosphere. Furthermore, acidic  
18 soils do not necessarily favour HONO emissions. Emissions are a factor of 700 higher  
19 for agricultural soils (Oswald et al., 2013), thus emissions might be highly influenced  
20 by microbial activities.
- 21 • NO<sub>2</sub> conversion on humic acid surfaces was found to be light-saturated from the early  
22 morning throughout most of the daytime under ambient conditions and, thus, only  
23 dependent on NO<sub>2</sub>. This saturation effect has not been observed in field measurements  
24 up to now. Consequently, we could not identify the expected correlation of HONO  
25 formation with  $j(\text{NO}_2)$  for this reaction. Furthermore, at low NO<sub>2</sub> levels this source is  
26 very small at our site.
- 27 • Photolysis of adsorbed HNO<sub>3</sub> was found to explain the estimated HONO fluxes when  
28 using an empirical parameterization for HONO formation, but it failed to produce  
29 noticeable amounts of HONO when the formation was calculated according to the  
30 proposed mechanism and literature values for adsorption cross sections and reaction  
31 kinetics.

1 Since HNO<sub>3</sub> photolysis is not correlated to  $j(\text{NO}_2)$  either, the correlation of the unknown  
2 HONO source to  $j(\text{NO}_2)$  as observed for example by Su et al. (2008) and Sörgel et al. (2011a)  
3 might originate from the unbalanced photolytic loss term of HONO ( $j(\text{HONO})_x[\text{HONO}]$ ).  
4 This loss term is highly correlated to  $j(\text{NO}_2)$  in the budget calculations (Oswald et al., 2014),  
5 and is generally interpreted as the unknown source. Recently, an internal source of HONO in  
6 the boundary layer from the interconversion between NO<sub>x</sub> and HO<sub>x</sub> has been postulated with a  
7 contribution of about 75 % (Li et al., 2014). Such a source would explain the observed  
8 correlation to  $j(\text{NO}_2)$  or  $j(\text{HONO})$ . In our study, the surface emission flux of HONO is only in  
9 the order of a few per cent of the calculated photolytic loss within the boundary layer, which  
10 is even less than estimated from boundary layer profile measurements (~20 % ground  
11 contribution; Zhang et al., 2009; Li et al., 2014).

12 However, a daytime ground source of HONO exists that can produce additional OH, thus  
13 enhancing the oxidation capacity of the lower troposphere. The relative contributions of  
14 ground sources and volume sources and, hence, the contribution of HONO to primary OH  
15 formation remains to be quantified by combining field measurements with the application of  
16 chemistry and transport models.

17

#### 18 **Acknowledgements:**

19 The authors gratefully acknowledge financial support by the German Science Foundation  
20 (DFG project HE 5214/4-1) and by the Max Planck Society. We would like to acknowledge  
21 the Department for Micrometeorology of the University of Bayreuth for the eddy flux  
22 measurements during IOP-3 and the meteorological data from the “Pflanzgarten”-site.  
23 Groundcover types and plant area data are courtesy of Eva Falge and Linda Voss. We are  
24 grateful to Robert Oswald for checking and assisting with the calculations regarding the soil  
25 emissions. Erica Duran helped with the nitrate loading sampling and calculated the needle  
26 areas. We thank Tracey Andreae for proofreading the manuscript.

27

#### 28 **References:**

29

- 30 Abida, O., Du, J., and Zhu, L.: Investigation of the photolysis of the surface-adsorbed HNO<sub>3</sub>  
31 by combining laser photolysis with Brewster angle cavity ring-down spectroscopy,  
32 Chem. Phys. Lett., 534, 77–82, 2012.  
33 Aliche, B., Geyer, A., Hofzumahaus, A., Holland, F., Konrad, S., Pätz, H. W., Schäfer, J.,  
34 Stutz, J., Volz-Thomas, A., and Platt, U.: OH formation by HONO photolysis during

- 1 the BERLIOZ experiment, *J. Geophys. Res.*, 108, 8247, doi:10.1029/2001JD000579,  
2 2003.
- 3 Allison F.: Losses of gaseous nitrogen from soils by chemical mechanisms involving nitrous  
4 acid and nitrites. *Soil Sci.*, 96, 404–409, 1963.
- 5 Amedro, D., Parker, A. E., Schoemaeker, C., and Fittschen, C.: Direct observation of OH  
6 radicals after 565 nm multi-photon excitation of NO<sub>2</sub> in the presence of H<sub>2</sub>O, *Chem.*  
7 *Phys. Lett.*, 513, 12–16, 2011.
- 8 Arens, F., Gutzwiller, L., Baltensperger, U. r., Gäggler, H. W., and Ammann, M.:  
9 Heterogeneous reaction of NO<sub>2</sub> on diesel soot particles, *Environ. Sci. Technol.*, 35,  
10 2191–2199, 2001.
- 11 Aubin, D. G., and Abbatt, J. P. D.: Interaction of NO<sub>2</sub> with hydrocarbon soot: focus on  
12 HONO yield, surface modification, and mechanism, *J. Phys. Chem. A*, 111, 6263–  
13 6273, 2007.
- 14 Bargsten, A., Falge, E., Pritsch, K., Huwe, B., and Meixner, F. X.: Laboratory measurements  
15 of nitric oxide release from forest soil with a thick organic layer under different  
16 understory types, *Biogeosciences*, 7, 1425–1441, doi:10.5194/bg-7-1425-2010, 2010.
- 17 Bartels-Rausch, T., Brigante, M., Elshorbany, Y. F., Ammann, M., D'Anna, B., George, C.,  
18 Stemmler, K., Ndour, M. and Kleffmann, J.: Humic acid in ice: Photo-enhanced  
19 conversion of nitrogen dioxide into nitrous acid, *Atmos. Environ.*, 44, 5443–5450,  
20 2010.
- 21 Bejan, I., Aal, Y. A. E., Barnes, I., Benter, T., Bohn, B., Wiesen, P., and Kleffmann, J.: The  
22 photolysis of ortho-nitrophenols: a new gas phase source of HONO, *Phys. Chem.*  
23 *Chem. Phys.*, 8, 2028–2035, DOI: 10.1039/b516590c, 2006.
- 24 Clark, F.E.: Losses of nitrogen accompanying nitrification. *Transactions of the International*  
25 *Society of Soil Science, Communications IV and V*, pp. 173–176, 1962.
- 26 Colussi, A. J., Enami, S., Yabushita, A., Hoffmann, M. R., Liu, W.-G., Mishraaf, H., and  
27 Goddard, W. A.: Tropospheric aerosol as a reactive intermediate, *Faraday Discuss.*,  
28 165, 407–420, 2013.
- 29 Cox, R. A.: The photolysis of nitrous acid in the presence of carbon monoxide and sulphur  
30 dioxide, *J. Photochem.*, 3, 291 - 304, 1974.
- 31 Crowley, J., N., and Carl, S., A.: OH formation in the photoexcitation of NO<sub>2</sub> beyond the  
32 dissociation threshold in the presence of water vapor, *J. Phys. Chem. A*, 101, 4178–  
33 4184, 1997.
- 34 De Boer, W. and Kowalchuk, G.A.: Nitrification in acid soils: micro-organisms and  
35 mechanisms, *Soil Biol. Biochem.*, 33, 853–866, 2001.
- 36 De Jesus Medeiros, D., and Pimentel, A. S.: New insights in the atmospheric HONO  
37 formation: New pathways for N<sub>2</sub>O<sub>4</sub> isomerization and NO<sub>2</sub> dimerization in the  
38 presence of water, *Journal of Physical Chemistry A*, 115, 6357–6365, 2011.
- 39 Donaldson, M. A., Berke, A. E., and Raff, J. D.: Uptake of Gas Phase Nitrous Acid onto  
40 Boundary Layer Soil Surfaces, *Environ. Sci. Technol.*, 48, 375–383, DOI:  
41 10.1021/es404156a, 2014a.
- 42 Donaldson, M. A., Bish, D. L., and Raff, J. D.: Soil surface acidity plays a determining role in  
43 the atmospheric-terrestrial exchange of nitrous acid, *P Natl Acad Sci USA*, 111,  
44 18472–18477, doi: 10.1073/pnas.1418545112, 2014b.
- 45 Febo, A., Perrino, C., and Allegrini, I.: Measurement of nitrous acid in Milan, Italy, by DOAS  
46 and diffusion denuders, *Atmos. Environ.*, 30 3599–3609, 1996.
- 47 Finlayson-Pitts, B. J., Wingen, L. M., Sumner, A. L., Syomin, D., and Ramazan, K. A.: The  
48 heterogeneous hydrolysis of NO<sub>2</sub> in laboratory systems and in outdoor and indoor  
49 atmospheres: An integrated mechanism, *Phys. Chem. Chem. Phys.*, 5, 2003.

- 1 Finlayson-Pitts, B. J.: Reactions at surfaces in the atmosphere: integration of experiments and  
2 theory as necessary (but not necessarily sufficient) for predicting the physical  
3 chemistry of aerosols, *Phys. Chem. Chem. Phys.*, 11, 7760–7779, 2009.
- 4 Foken, T.: Lufthygienisch-bioklimatische Kennzeichnung des oberen Egertales  
5 (Fichtelgebirge bis Karlovy Vary). *Bayreuther Forum Ökologie*, 100, Bayreuth, 70  
6 pp., 2003.
- 7 Foken, T.: *Micrometeorology*, Springer, Heidelberg, 308 pp., 2008.
- 8 Foken, T., Meixner, F. X., Falge, E., Zetzsch, C., Serafimovich, A., Bargsten, A., Behrendt,  
9 T., Biermann, T., Breuninger, C., Dix, S., Gerken, T., Hunner, M., Lehmann-Pape, L.,  
10 Hens, K., Jocher, G., Kesselmeier, J., Lüers, J., Mayer, J.-C., Moravek, A., Plake, D.,  
11 Riederer, M., Rütz, F., Scheibe, M., Siebicke, L., Sörgel, M., Staudt, K., Trebs, I.,  
12 Tsokankunku, A., Welling, M., Wolff, V., and Zhu, Z.: Coupling processes and  
13 exchange of energy and reactive and non-reactive trace gases at a forest site – results  
14 of the EGER experiment, *Atmos. Chem. Phys.*, 12, 1923–1950, doi:10.5194/acp-12-  
15 1923-2012, 2012.
- 16 George, C., Streckowski, R. S., Kleffmann, J., Stemmler, K., and Ammann, M.:  
17 Photoenhanced uptake of gaseous NO<sub>2</sub> on solid organic compounds: a photochemical  
18 source of HONO?, *Faraday Discuss.*, 130, 195–210, 2005.
- 19 Gustafsson, R. J., Kyriakou, G., and Lambert, R. M.: The molecular mechanism of  
20 tropospheric nitrous acid production on mineral dust surfaces, *ChemPhysChem*, 9,  
21 1390–1393, 2008.
- 22 Gutzwiller, L., George, C., Rössler, E., and Ammann, M.: Reaction kinetics of NO<sub>2</sub> with  
23 resorcinol and 2,7-naphthalenediol in the aqueous phase at different pH, *J. Phys.*  
24 *Chem. A*, 106, 12045–12050, 2002.
- 25 Harrison, R. M., and Kitto, A.-M. N.: Evidence for a surface source of atmospheric nitrous  
26 acid, *Atmos. Environ.*, 28, 1089–1094, 1994.
- 27 Harrison, R. M., Peak, J. D., and Collin, G. M.: Tropospheric cycle of nitrous acid, *J.*  
28 *Geophys. Res.*, 101, 14429–14439, 1996.
- 29 Heland, J., Kleffmann, J., Kurtenbach, R., and Wiesen, P.: A new instrument to measure  
30 gaseous nitrous acid (HONO) in the atmosphere, *Environ. Sci. Technol.*, 35, 3207–  
31 3212, 2001.
- 32 Kamboures, M. A., Raff, J. D., Miller, Y., Phillips, L. F., Finlayson-Pitts, B. J., and Gerber,  
33 R. B.: Complexes of HNO<sub>3</sub> and NO<sub>3</sub> with NO<sub>2</sub> and N<sub>2</sub>O<sub>4</sub>, and their potential role in  
34 atmospheric HONO formation, *Phys. Chem. Chem. Phys.*, 10, 6019–6032, 2008.
- 35 Kleffmann, J., Becker, K. H., Lackhoff, M., and Wiesen, P.: Heterogeneous conversion of  
36 NO<sub>2</sub> on carbonaceous surfaces, *Phys. Chem. Chem. Phys.*, 1, 5443–5450, 1999.
- 37 Kleffmann, J., Heland, J., Kurtenbach, R., Lörzer, J., and Wiesen, P.: A new instrument  
38 (LOPAP) for the detection of nitrous acid (HONO), *Environ. Sci. Pollut. R.*, 4, 48–54,  
39 2002.
- 40 Kleffmann, J., Gavriloaiei, T., Hofzumahaus, A., Holland, F., Koppmann, R., Rupp, L.,  
41 Schlosser, E., Siese, M., and Wahner, A.: Daytime formation of nitrous acid: A major  
42 source of OH radicals in a forest, *Geophys. Res. Lett.*, 32, 2005.
- 43 Kleffmann, J.: Daytime sources of nitrous acid (HONO) in the atmospheric boundary layer,  
44 *ChemPhysChem*, 8, 1137 – 1144, 2007.
- 45 Kubota, M. and Asami, T.: Source of nitrous acid volatilized from upland soils, *Soil Sci. Plant*  
46 *Nutr.*, 31, 35–42, 1985.
- 47 Lee, B.H, Wood, E. C., Herndon, S. C., Lefer, B. L., Luke, W. T., Brune, W. H., Nelson, D.  
48 D., Zahniser, M. S. and Munger, J. W.: Urban measurements of atmospheric nitrous  
49 acid: A caveat on the interpretation of the HONO photostationary state, *J. Geophys.*  
50 *Res.*, 118, 1–8, doi:10.1002/2013JD020341, 2013.

- 1 Li, X., Rohrer, F., Hofzumahaus, H., Brauers, T., Häseler, R., Bohn, B., Broch, S., Fuchs, H.,  
2 Gomm, S., Holland, F., Jäger, J., Kaiser, J., Keutsch, F. N., Lohse, I., Lu, K.,  
3 Tillmann, R., Wegener, R., Wolfe, G. M., F. Mentel, T. F., Kiendler-Scharr, A. and  
4 Wahner, A.: Missing gas-phase source of HONO inferred from zeppelin  
5 measurements in the troposphere, *Science*, 344, 292, 2014.
- 6 Ludwig, J., Meixner, F. X., Vogel, B. and Förstner J.: Soil-air exchange of nitric oxide: An  
7 overview of processes, environmental factors, and modeling studies, *Biogeochemistry*,  
8 52, 225–257, 2001.
- 9 Madronich, S. and Flocke, S., The role of solar radiation in atmospheric chemistry, in *The*  
10 *Handbook of Environmental Chemistry / Reactions and Processes / Environmental*  
11 *Photochemistry Part I: BD 2 / Part L*, Boule, P. (ed.), Springer-Verlag, Heidelberg,  
12 373 (pp. 1-26), 1998.
- 13 Maljanen, M., Yli-Pirilä, P., Hytönen, J., Joutsensaari, J., and Martikainen, P. J.: Acidic  
14 northern soils as sources of atmospheric nitrous acid (HONO), *Soil Biol. Biochem.*,  
15 67, 94–97, DOI: 10.1016/j.soilbio.2013.08.013, 2013.
- 16 Matthies, C., Erhard, H.-P., Drake, H.L.: Effects of pH on the comparative culturability of  
17 fungi and bacteria from acidic and less acidic forest soils, *J. Basic. Microb.*, 37, 335-  
18 343, 1997.
- 19 Mauder, M. and Foken, T.: Documentation and instruction manual of the eddy-covariance  
20 software package TK3, Universität Bayreuth, Abteilung Mikrometeorologie, 46, 60  
21 pp., ISSN1614-8924, 2011.
- 22 Miller, Y., Finlayson-Pitts, B. J., and Gerber, R. B.: Ionization of N<sub>2</sub>O<sub>4</sub> in contact with water:  
23 mechanism, time scales and atmospheric implications, *J. Am. Chem. Soc.*, 131,  
24 12180–12185, DOI: 10.1021/ja900350g, 2009.
- 25 Moldrup, P., Olesen, T., Gamst, J., Schjonning, P., Yamaguchi, T., and Rolston, D. E.:  
26 Predicting the gas diffusion coefficient in repacked soil: Water-induced linear  
27 reduction model, *Soil Science Society of America Journal*, 64, 1588-1594, 2000.
- 28 Oswald, R., Behrendt, T., Ermel, M., Wu, D., Su, H., Cheng, Y., Breuninger, C., Moravek,  
29 A., Mougou, Delon, C., Loubet, B., Pommerening-Röser, A., Sörgel, M., Pöschl, U.,  
30 Hoffmann, T., Andreae, M.O., Meixner, F.X. and Trebs, I.: HONO emissions from  
31 soil bacteria as a major source of atmospheric reactive Nitrogen, *Science*, 341, 1233-  
32 1235, DOI: 10.1126/science.1242266, 2013.
- 33 Oswald, R., Ermel, M., Hens, K., Novelli, A., Ouwersloot, H. G., Paasonen, P., Petäjä, T.,  
34 Sipilä, M., Keronen, P., Bäck, J., Königstedt, R., Hosaynali Beygi, Z., Fischer, H.,  
35 Bohn, B., Kubistin, D., Harder, H., Martinez, M., Williams, J., Hoffmann, T., Trebs,  
36 I., and Sörgel, M.: Comparison of HONO budgets for two measurement heights at a  
37 field station within the boreal forest (SMEAR II – HUMPPA-COPEC 2010), *Atmos.*  
38 *Chem. Phys. Discuss.*, 14, 7823-7857, doi:10.5194/acpd-14-7823-2014, 2014.
- 39 Oren, R., Schulze, E.-D., Matyssek, R., and Zimmermann, R.: Estimating photosynthetic rate  
40 and annual carbon gain in conifers from specific leaf weight and leaf biomass,  
41 *Oecologia*, 70, 187– 193, 1986.
- 42 Pape, L., Ammann, C., Nyfeler-Brunner, A., Spirig, C., Hens, K., and Meixner, F. X.: An  
43 automated dynamic chamber system for surface exchange measurement of non-  
44 reactive and reactive trace gases of grassland ecosystems, *Biogeosciences*, 6, 405-429,  
45 doi:10.5194/bg-6-405-2009, 2009.
- 46 Ramazan, K. A., Syomin, D., Finlayson-Pitts, B. J.: The photochemical production of HONO  
47 during the heterogeneous hydrolysis of NO<sub>2</sub>. *Phys. Chem. Chem. Phys.*, 6, 3836-3843,  
48 2004.
- 49 Ren, X., Sanders, J. E., Rajendran, A., Weber, R. J., Goldstein, A. H., Pusede, S. E., Browne,  
50 E. C., Min, K.-E., and Cohen, R. C.: A relaxed eddy accumulation system for



- 1 measuring vertical fluxes of nitrous acid, *Atmos. Meas. Tech.*, 4, 2093-2103,  
2 doi:10.5194/amt-4-2093-2011, 2011.
- 3 Rousk, J., Bååth, E., Brookes, P.C., Lauber, C.L., Lozupone, C., Caporaso, J.G., Knight, R.,  
4 and Fierer, N.: Soil bacterial and fungal communities across a pH gradient in an arable  
5 soil, *ISME J.*, 4, 1340–1351, 2010.
- 6 Rubasinghege, G., and Grassian V. H.: Photochemistry of adsorbed nitrate on aluminum  
7 oxide particle surfaces, *J. Phys. Chem. A*, 113, 7818–7825, 2009.
- 8 Scharko, N. K., Berke, A. E., and Raff, J. D.: Release of nitrous acid and nitrogen dioxide  
9 from nitrate photolysis in acidic aqueous solutions, *Environ. Sci. Technol.*, 48, 11991–  
10 12001, doi: 10.1021/es503088x, 2014.
- 11 Schimang R., Folkers A., Kleffmann J., Kleist E., Miebach M., Wildt J.: Uptake of Gaseous  
12 Nitrous Acid (HONO) by Several Plant Species, *Atmos. Environ.*, 40, 1324-1335,  
13 2006.
- 14 Schuttelfield, J., Rubasinghege, G., El-Maazawi, M., Bone, J., and Grassian V. H.:  
15 Photochemistry of adsorbed nitrate, *J. Am. Chem. Soc.*, 130, 12210–12211, 2008.
- 16 Sörgel, M., Regelin, E., Bozem, H., Diesch, J.-M., Drewnick, F., Fischer, H., Harder, H.,  
17 Held, A., Hosaynali-Beygi, Z., Martinez, M., and Zetzsch, C.: Quantification of the  
18 unknown HONO daytime source and its relation to NO<sub>2</sub>, *Atmos. Chem. Phys.*, 11,  
19 10433-10447, doi:10.5194/acp-11-10433-2011, 2011a.
- 20 Sörgel, M., Trebs, I., Serafimovich, A., Moravek, A., Held, A., and Zetzsch, C.: Simultaneous  
21 HONO measurements in and above a forest canopy: influence of turbulent exchange  
22 on mixing ratio differences, *Atmos. Chem. Phys.*, 11, 841-855, doi:10.5194/acp-11-  
23 841-2011, 2011b.
- 24 Stemmler, K., Ammann, M., Donders, C., Kleffmann, J., and George, C.: Photosensitized  
25 reduction of nitrogen dioxide on humic acid as a source of nitrous acid, *Nature*, 440,  
26 195-198, 2006.
- 27 Stemmler, K., Ammann, M., Elshorbany, Y., Kleffmann, J., Ndour, M., D’Anna, B., George,  
28 C., and Bohn, B.: Light induced conversion of nitrogen dioxide into nitrous acid on  
29 submicron humic acid aerosol, *Atmos. Chem. Phys.*, 7, 4237–4248, 2007.
- 30 Stutz, J., Alicke, B., and Neftel, A.: Nitrous acid formation in the urban atmosphere: Gradient  
31 measurements of NO<sub>2</sub> and HONO over grass in Milan, Italy, *J. Geophys. Res.*, 107  
32 doi:10.1029/2001JD000390, 2002.
- 33 Su, H., Cheng, Y. F., Shao, M., Gao, D. F., Yu, Z. Y., Zeng, L. M., Slanina, J., Zhang, Y. H.,  
34 and Wiedensohler, A.: Nitrous acid (HONO) and its daytime sources at a rural site  
35 during the 2004 PRIDE-PRD experiment in China, *J. Geophys. Res.*, 113,  
36 doi:10.1029/2007JD009060, 2008.
- 37 Su, H., Cheng, Y., Oswald, R., Behrendt, T., Trebs, I., Meixner, F.-X., Andreae, M. O.,  
38 Cheng, P., Zhang, Y., and Pöschl, U.: Soil nitrite as a source of atmospheric HONO  
39 and OH radicals, *Science*, 333, 1616–1618, doi:10.1126/science.1207687, 2011.
- 40 Trebs, I., Bohn, B., Ammann, C., Rummel, U., Blumthaler, M., Königstedt, R., Meixner, F.  
41 X., Fan, S., and Andreae, M. O.: Relationship between the NO<sub>2</sub> photolysis frequency  
42 and the solar global irradiance, *Atmos. Meas. Tech.*, 2, 725–739, 2009.
- 43 Van Cleemput, O. and Baert, L.: Nitrite: a key compound in N loss processes under acid  
44 conditions?, *Plant Soil*, 76, 233-241, 1984.
- 45 VandenBoer, T. C., Brown, S. S., Murphy, J. G., Keene, W. C., Young, C. J., Pszenny, A. A.  
46 P., Kim, S., Warneke, C., de Gouw, J. A., Maben, J. R., Wagner, N. L., Riedel, T. P.,  
47 Thornton, J. A., Wolfe, D. E., Dubé, W. P., Öztürk, F., Brock, C. A., Grossberg, N.,  
48 Lerner, B., Lerner, B., Middlebrook, A. M., and Roberts, J. M.: Understanding the role  
49 of the ground surface in HONO vertical structure: High resolution vertical profiles

1 during NACHTT-11, *Journal of Geophysical Research: Atmospheres*, 118, 10,155-  
2 110,171, 10.1002/jgrd.50721, 2013.

3 VandenBoer, T. C., Young, C. J., Talukdar, R. K., Markovic, M. Z., Brown, S. S., Roberts, J.  
4 M., and Murphy, J. G.: Nocturnal loss and daytime source of nitrous acid through  
5 reactive uptake and displacement, *Nat. Geosci.*, 8, 5-7, doi:10.1038/ngeo2315, 2015.

6 Venterea, R.T., Rolston, D.E., and Cardon, Z.G.: Effects of soil moisture, physical, and  
7 chemical characteristics on abiotic nitric oxide production, *Nutr. Cycl. Agroecosys.*,  
8 72, 27–40, 2005.

9 Volkamer, R., Sheehy, P., Molina, L. T., and Molina, M. J.: Oxidative capacity of the Mexico  
10 City atmosphere – Part 1: A radical source perspective, *Atmos. Chem. Phys.*, 10,  
11 6969–6991, doi:10.5194/acp-10-6969-2010, 2010.

12 Wolff, V., Trebs, I., Ammann, C., and Meixner, F. X.: Aerodynamic gradient measurements  
13 of the  $\text{NH}_3\text{-HNO}_3\text{-NH}_4\text{NO}_3$  triad using a wet chemical instrument: an analysis of  
14 precision requirements and flux errors, *Atmos. Meas. Tech.*, 3, 187-208,  
15 doi:10.5194/amt-3-187-2010, 2010.

16 Wong, K. W., Oh, H.-J., Lefer, B. L., Rappenglück, B., and Stutz, J.: Vertical profiles of  
17 nitrous acid in the nocturnal urban atmosphere of Houston, TX, *Atmos. Chem. Phys.*,  
18 11, 3595-3609, doi:10.5194/acp-11-3595-2011, 2011.

19 Wong, K. W., Tsai, C., Lefer, B., Haman, C., Grossberg, N., Brune, W. H., Ren, X., Luke,  
20 W., and Stutz, J.: Daytime HONO vertical gradients during SHARP 2009 in Houston,  
21 TX, *Atmos. Chem. Phys.*, 12, 635-652, doi:10.5194/acp-12-635-2012, 2012.

22 Wong, K. W., Tsai, C., Lefer, B., Grossberg, N., and Stutz, J.: Modeling of daytime HONO  
23 vertical gradients during SHARP 2009, *Atmos. Chem. Phys.*, 13, 3587-3601,  
24 10.5194/acp-13-3587-2013, 2013.

25 Yabushita, A., Enami, S., Sakamoto, Y., Kawasaki, M., Hoffmann, M. R., and Colussi, A. J.:  
26 Anion-catalyzed dissolution of  $\text{NO}_2$  on aqueous microdroplets, *J. Phys. Chem. A*, 113,  
27 4844–4848, 2009.

28 Zhang, N., Zhou, X., Shepson, P. B., Gao, H., Alaghmand, M., and Stirm, B.: Aircraft  
29 measurement of HONO vertical profiles over a forested region, *Geophys. Res. Lett.*,  
30 36, L15820, doi:10.1029/2009GL038999, 2009.

31 Zhang, N., Zhou, X., Bertman, S., Tang, D., Alaghmand, M., Shepson, P. B., and Carroll, M.  
32 A.: Measurements of ambient HONO concentrations and vertical HONO flux above a  
33 northern Michigan forest canopy, *Atmos. Chem. Phys.*, 12, 8285-8296,  
34 doi:10.5194/acp-12-8285-2012, 2012.

35 Zhou, X., He, Y., Huang, G., Thornberry, T. D., Carroll, M. A., and Bertman, S. B.:  
36 Photochemical production of nitrous acid on glass sample manifold surface, *Geophys.*  
37 *Res. Lett.*, 29, 1681, 10.1029/2002GL015080, 2002.

38 Zhou, X., Gao, H., He, Y., Huang, G., Bertman, S. B., Civerolo, K., and Schwab, J.: Nitric  
39 acid photolysis on surfaces in low-NO<sub>x</sub> environments: Significant atmospheric  
40 implications, *Geophys. Res. Lett.*, 30, 1-4, 2003.

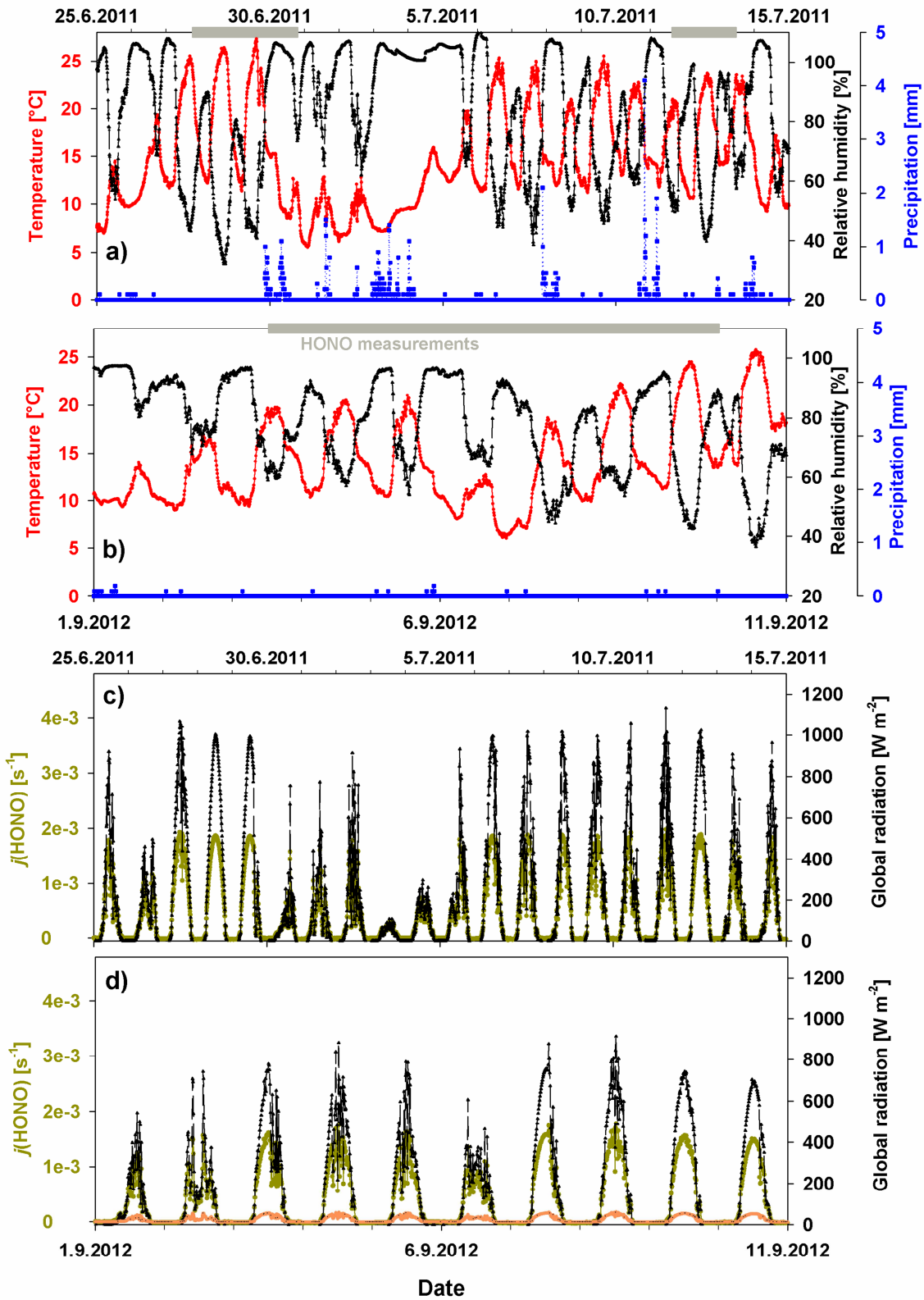
41 Zhou, X. L., Zhang, N., TerAvest, M., Tang, D., Hou, J., Bertman, S., Alaghmand, M.,  
42 Shepson, P. B., Carroll, M. A., Griffith, S., Dusanter, S., and Stevens, P. S.: Nitric acid  
43 photolysis on forest canopy surface as a source for tropospheric nitrous acid, *Nat.*  
44 *Geosci.*, 4, 440-443, 10.1038/ngeo1164, 2011.

45 Zhu, C., Xiang, B., Zhu, L., Cole, R.: Determination of absorption cross sections of surface-  
46 adsorbed  $\text{HNO}_3$  in the 290–330 nm region by Brewster angle cavity ring-down  
47 spectroscopy, *Chem. Phys. Lett.*, 458, 73–377, 2008.

48 Zhu, C., Xiang, B., Chu, L. T. and Zhu, L.: Photolysis of Nitric Acid in the Gas Phase, on  
49 Aluminum Surfaces, and on Ice Films, *J. Phys. Chem. A*, 114, 2561–2568, 2010.

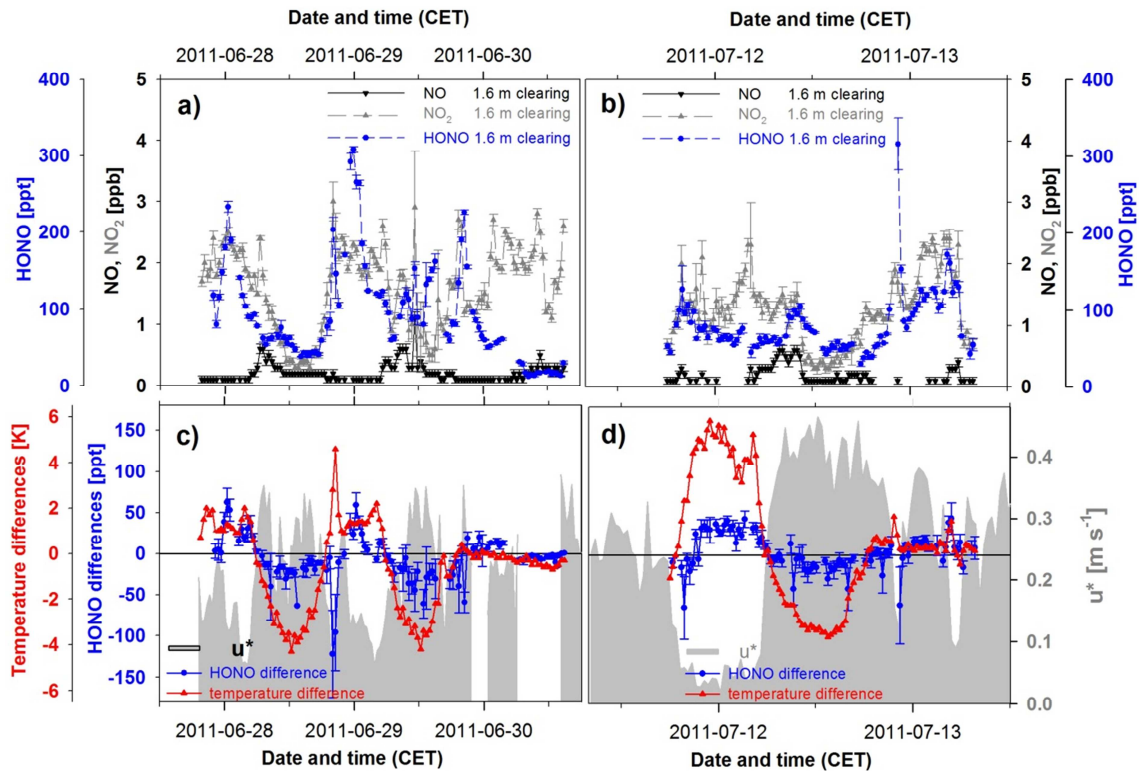
50

1  
2

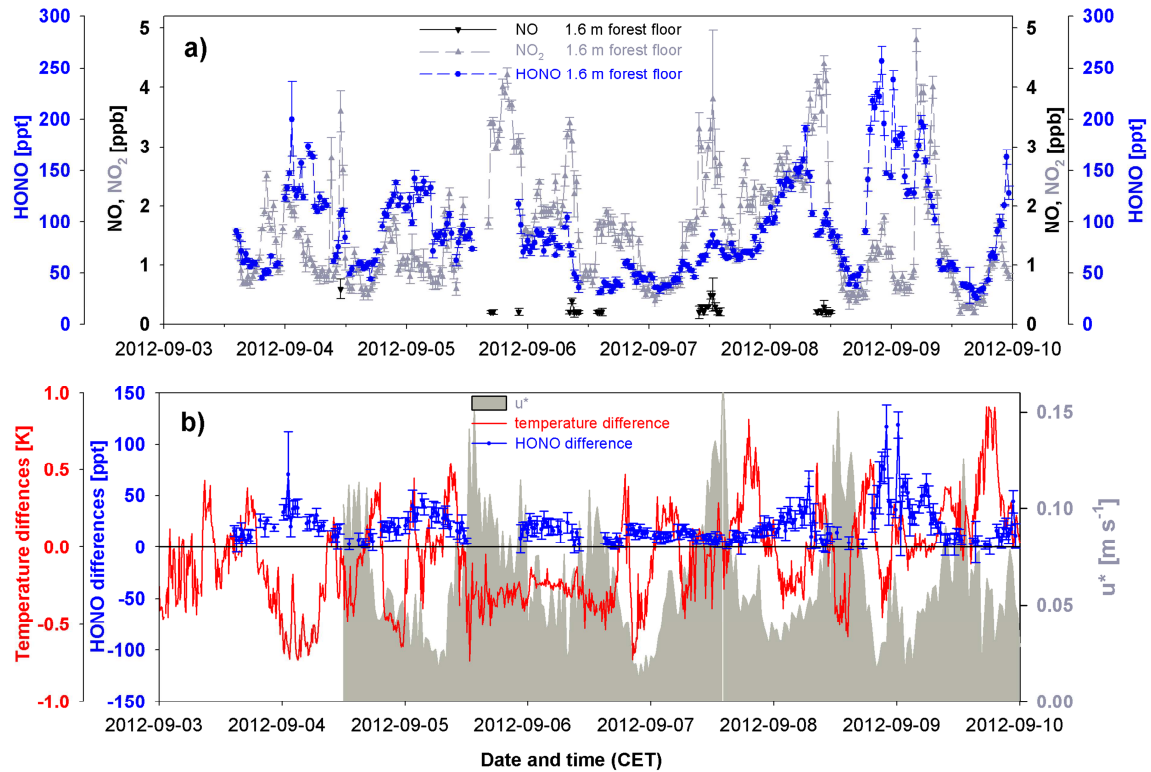


3

1 Figure 1: Temperature (red), relative humidity (RH, black) and precipitation (blue) averaged for a 10 min  
 2 interval are shown in panels a) for 25<sup>th</sup> June to 15<sup>th</sup> July 2011 (IOP-3), and b) for 1<sup>st</sup> September 2012 to 11<sup>th</sup>  
 3 September 2012 (IOP-4). Periods when HONO vertical profiles were measured are indicated by grey bars at the  
 4 top of the graphs. Panels c) and d) show solar global irradiance (black) and  $j(\text{HONO})$  in dark yellow, calculated  
 5 according to Trebs et al. (2009), for the respective campaigns. Additionally,  $j(\text{HONO})$  at the forest floor (orange)  
 6 was calculated by applying a factor of 10 taking into account attenuation by the canopy (cf. Sörgel et al., 2011b).  
 7 All data were taken from the “Pflanzgarten” site.  
 8  
 9

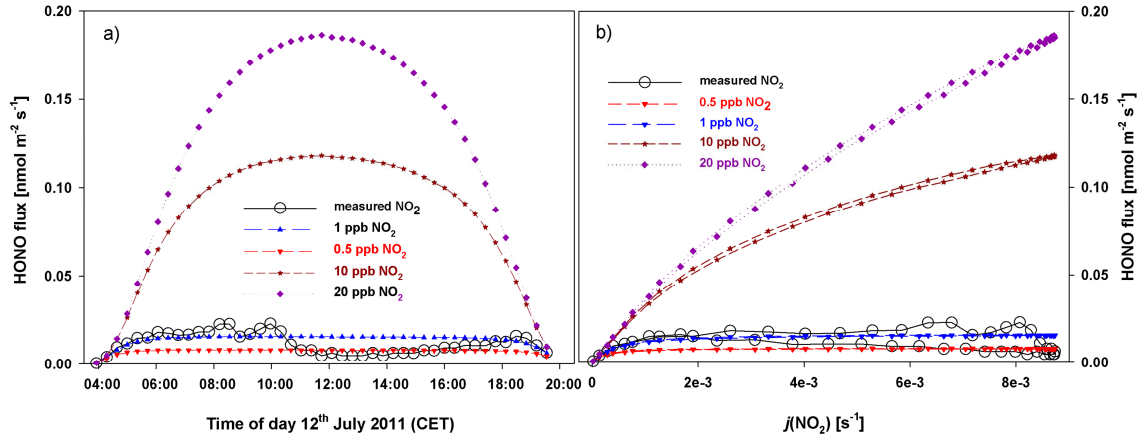


10  
 11 Figure 2: HONO (blue), NO (black) and NO<sub>2</sub> (grey) mixing ratios measured at the clearing at 1.6 m averaged for  
 12 each height interval (i.e. omitting the first data points according to the time resolution of the instruments) from a)  
 13 27 June to 30 June 2011 (NOx: 3.5 min mean; HONO: 3 min mean), and b) 11 July to 13 July 2011 (NOx: 4 min  
 14 mean; HONO: 3 min mean). Missing NO values are below the detection limit ( $\text{LOD}_{2\sigma} = 50$  ppt). Vertical  
 15 temperature differences (red triangles and line) and HONO mixing ratio differences (blue dots and line) for each  
 16 cycle (~ 30 min) are shown in c) and d) as well as the friction velocity (30 min mean) in grey shading.  
 17 Differences of mean HONO values measured at 1.6 m and 0.1 m are presented and error bars denote combined  
 18 standard deviations. For temperature, differences between 1.4 m and 0.1 m are shown.  
 19



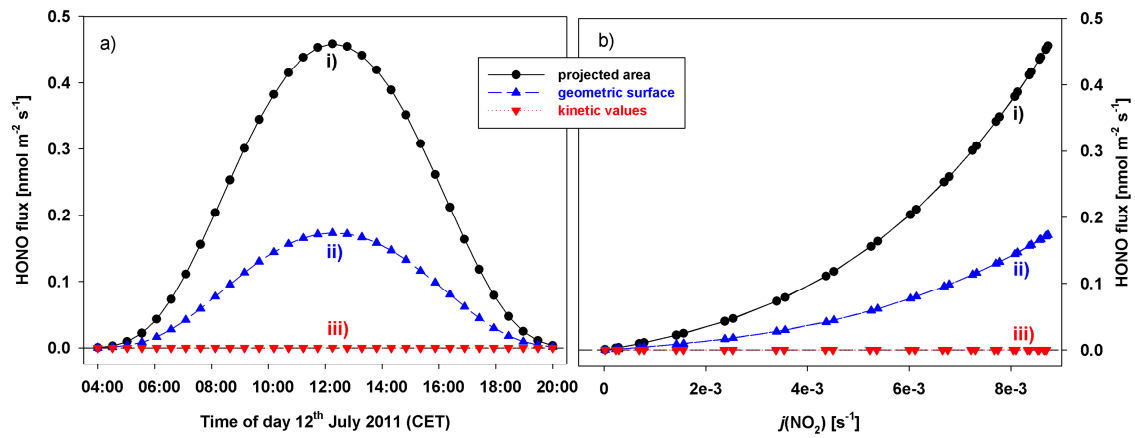
1  
2  
3  
4  
5  
6  
7  
8  
9  
10

Figure 3: HONO (blue), NO (black) and NO<sub>2</sub> (grey) mixing ratios measured at the forest floor at 1.6 m averaged for each height interval (i.e. omitting the first data points according to the time resolution of the instruments) from 3 September to 9 Sept 2012 (NOx: 7 min mean; HONO: 6 min mean) are shown in a). Missing NO values are below the detection limit ( $\text{LOD}_{2\sigma} = 50$  ppt). Vertical temperature differences (red triangles and line) and HONO mixing ratio differences (blue dots and line) for each cycle (~ 30 min) are shown in b) as well as the friction velocity (30 min mean) in grey shading. Differences of mean HONO values measured at 1.6 m and 0.1 m are presented and error bars denote combined standard deviations. For temperature, differences between 1.6 m and 0.1 m are shown.



1  
2  
3  
4  
5  
6

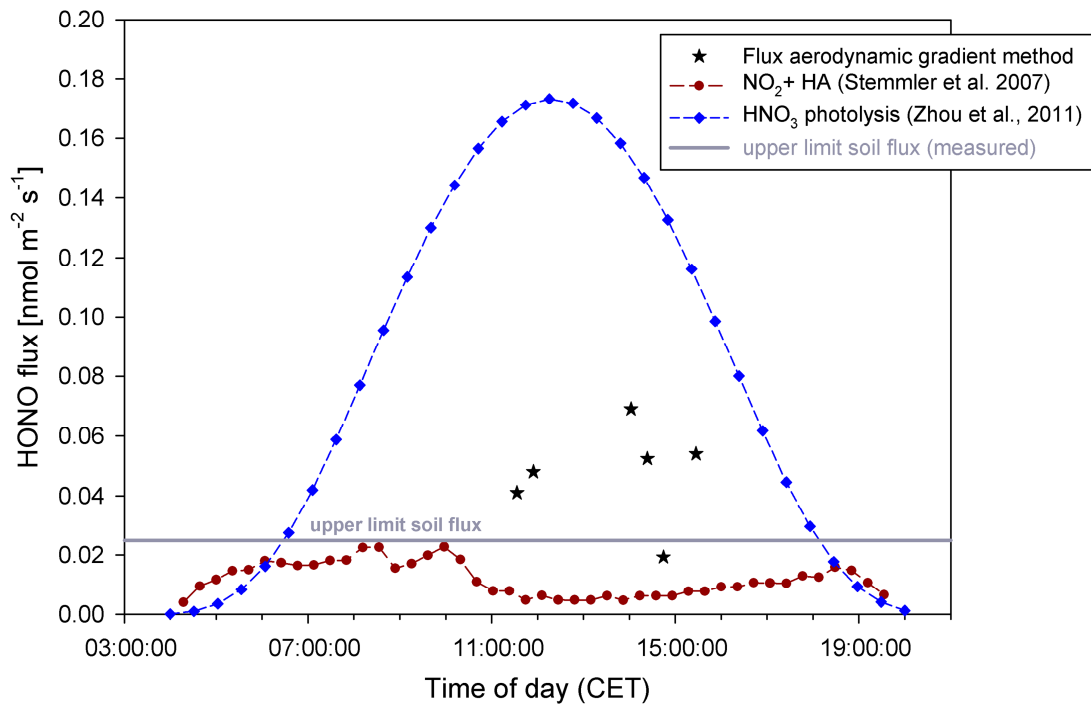
Figure 4: Diurnal cycles of HONO emission fluxes caused by light induced NO<sub>2</sub> conversion for different NO<sub>2</sub> mixing ratios are shown in a). The corresponding correlations of HONO formation with  $j(\text{NO}_2)$  are presented in b).



7  
8  
9  
10  
11

Figure 5: HONO fluxes from photolysis of adsorbed HNO<sub>3</sub> calculated by three different approaches (for details see text). Diurnal cycles of the HONO fluxes are shown in a), whereas b) shows the relationship between HONO fluxes and  $j(\text{NO}_2)$ .

## HONO fluxes at clearing (12<sup>th</sup> July 2011)



1

2

Figure 6: Comparison of measured HONO fluxes at the clearing on 12 July 2012 with estimates of potential HONO sources. Black stars represent the fluxes derived from the aerodynamic gradient method. Blue diamonds are HONO fluxes calculated from the measured nitrate loadings according to Zhou et al. (2011) but using the geometric needle area (see Sect. 3.4.3, approach ii). Brown dots are calculated HONO fluxes according to Stemmler et al. (2007) assuming a flat surface covered with humic acid. The grey horizontal line marks the upper limit of soil HONO fluxes derived from laboratory dynamic chamber measurements.

3

4

5

6

7

8